Analytically solvable two-level quantum systems and Landau-Zener interferometry

Edwin Barnes[*]

Condensed Matter Theory Center, Department of Physics, University of Maryland, College Park, Maryland 20742-4111, USA

(Received 13 December 2012; published 15 July 2013)

A simple algorithm is presented based on a type of partial reverse engineering that generates an unlimited number of exact analytical solutions to the Schrödinger equation for a general time-dependent two-level Hamiltonian. I demonstrate this method by deriving exact solutions corresponding to fast control pulses that contain arbitrarily many tunable parameters. It is shown that the formalism is naturally suited to generating analytical control protocols that perform precise nonadiabatic rapid passage and Landau-Zener interferometry near the quantum speed limit. A general, exact formula for Landau-Zener interference patterns is derived.

DOI: 10.1103/PhysRevA.88.013818 PACS number(s): 42.50.Ct, 03.65.Aa, 03.67.Ac, 07.05.Dz

I. INTRODUCTION

Although they have pervaded quantum physics since its inception, very few time-dependent two-level quantum systems are known to be analytically solvable. Among the most famous examples of exactly soluble two-level evolution is the Landau-Majorana-Stückelberg-Zener (LMSZ) problem [1–5], which remains a very active area of research due to numerous applications pertaining to quantum phase transitions [6], quantum control [7–11], and quantum state preparation [12–14]. The hyperbolic secant pulse of Rosen and Zener [15] has played an important role in self-induced transparency [16] and qubit control [17–19], and it has since been found to belong to a larger family of analytical controls [20–30]. Several of these examples have proven very beneficial to the fields of quantum control and computation [17,18,31–34], where analytical solutions are often central in the design of control fields that are fast, precise, and robust against noise. However, the rarity of such solutions has severely limited one's options in developing an analytical approach to qubit gate design.

In a recent work [35], a systematic method for deriving arbitrarily many families of exactly solvable two-state systems was presented, vastly extending the number of known analytical solutions. This method allows one to input many of the basic features of the desired control field and then compute exactly the corresponding evolution of the system with the provided formulas. However, a limitation of this work is that it applies only to systems where the driving is along a single axis of the Bloch sphere, such as in the case of electrically driven singlet-triplet qubits [36–39], making it inapplicable to the majority of driven two-level systems.

In this paper, I address this limitation by presenting a method to generate arbitrarily many families of solutions in the most general case where the two-level Hamiltonian has time dependence along any set of axes of the Bloch sphere. Of course, one can easily generate exactly solvable Hamiltonians by first choosing the evolution operator and then differentiating to obtain the corresponding Hamiltonian, but it is challenging to arrive at a physically meaningful Hamiltonian in this way. In contrast, the method presented here allows one to specify the basic form and many features of the Hamiltonian whose evolution one wishes to solve before proceeding to compute the exact solution for this evolution. This method has important applications in a vast range of problems, including the development of quantum controls for essentially any quantum computing platform and control protocols for performing LMSZ interferometry and nonadiabatic rapid passage (NARP). I illustrate this by deriving exactly solvable LMSZ driving fields and control pulses that execute a desired evolution at speeds approaching the quantum speed limit (QSL) [40–46]. Attaining fast evolution times is especially crucial in quantum computing where quantum gates need to be performed on time scales much shorter than the decoherence time. In the case of periodic driving through a level anticrossing, I show that the formalism allows one to easily derive analytical expressions for LMSZ interference patterns and conditions for coherent destruction of tunneling [47,48].

II. ANALYTICALLY SOLVABLE HAMILTONIANS

The Hamiltonian we consider has the general form

$$H = b_x(t)\sigma_x + b_y(t)\sigma_y + b_z(t)\sigma_z, \tag{1}$$

where the $b_k(t)$ are real functions and the σ_k are Pauli matrices. This Hamiltonian describes any time-dependent two-level system, with the functions $b_k(t)$ interpreted as either driving fields or time-dependent energy splittings. Alternatively, we may parametrize the Hamiltonian in terms of rotating-frame fields α, β, and φ, where $\beta e^{i\varphi} \equiv b_x + i b_y$ and $\alpha(t) \equiv 2\int_0^t dt' b_z(t') - \varphi(t)$. In the Appendix, it is shown that one can systematically find analytical solutions for the evolution operator generated by Hamiltonian (1) with φ and either α or β chosen as desired; although one cannot choose both α and β at will (were this the case, all two-state problems could be solved analytically), one still has a large amount of control over the features of the second, unspecified function. For concreteness, we suppose that one wishes to fix $\beta(t)$ at the outset [the formalism can easily be modified to fix $\alpha(t)$ instead]. While we cannot then find analytical solutions for arbitrary α, there exists a different parametrization of the Hamiltonian in which α is replaced with a new function, $\chi(t)$, such that one can systematically generate an analytical expression for the evolution operator for arbitrary choices of β, φ, and χ. Parametrizing the laboratory-frame evolution

[*]barnes@umd.edu

operator as

$$U = \begin{pmatrix} u_{11} & -u_{21}^* \\ u_{21} & u_{11}^* \end{pmatrix}, \quad |u_{11}|^2 + |u_{21}|^2 = 1, \tag{2}$$

the explicit u_{11}, u_{21} and driving fields are (see the Appendix)

$$u_{11} = \cos\chi\, e^{i\xi_- - i\varphi/2}, \quad u_{21} = i\eta \sin\chi\, e^{i\xi_+ + i\varphi/2}, \tag{3}$$

$$\xi_\pm = \int_0^t dt'\beta\sqrt{1 - \frac{\dot\chi^2}{\beta^2}}\csc(2\chi) \pm \frac{1}{2}\sin^{-1}\left(\frac{\dot\chi}{\beta}\right) \pm \eta\frac{\pi}{4},$$
$$b_x = \beta\cos\varphi, \quad b_y = \beta\sin\varphi, \tag{4}$$
$$b_z = \frac{\ddot\chi - \dot\chi\dot\beta/\beta}{2\beta\sqrt{1-\dot\chi^2/\beta^2}} - \beta\sqrt{1-\dot\chi^2/\beta^2}\cot(2\chi) + \frac{\dot\varphi}{2}.$$

The initial conditions $u_{11}(0) = 1$, $u_{21}(0) = 0$ imply $\chi(0) = 0$, and $\dot\chi(0) = -\eta\beta(0)$ ensures that $b_z(0)$ is finite, where $\eta = \pm 1$. Equations (3) and (4) embody one of the main results of this paper, as they constitute a general analytic solution of the evolution generated by the Hamiltonian of Eq. (1). The task of finding analytical solutions has been reduced to first choosing b_x, b_y by picking β and φ at will. One then selects χ to produce a desired b_z via Eq. (4), fixing the Hamiltonian. Once these choices are made, an analytical expression for the evolution operator follows from Eq. (3). A simple case is $\chi = -\eta\int_0^t dt'\beta(t')$ and $\varphi = 0$, where Eq. (4) gives that $b_y = b_z = 0$, corresponding to an x rotation for any β. Another simple example arises when $\beta = \chi = 0$, for which Eq. (3) yields a z rotation for any b_z.

III. QUANTUM SPEED LIMIT

In Eqs. (3) and (4), it is clear that proper solutions necessarily satisfy $|\dot\chi| \leqslant |\beta|$. The physical origin of this constraint lies in the notion of the QSL [40–46], which refers to the minimum time it takes a quantum state to evolve to a different state in the Hilbert space due to energy-time uncertainty. Indeed, $|\dot\chi| \leqslant |\beta|$ implies that the fastest possible evolution from $\chi(0) = 0$ to a desired final value $\chi_{\text{target}} \equiv \chi(T) > 0$ is obtained by choosing $\chi(t) = \int_0^t dt'|\beta(t')|$, with the shortest time given by substituting $t = T$ in this expression and solving for T in terms of χ_{target} and whatever parameters might appear in β. For constant $\beta = \beta_0 > 0$, we immediately obtain $T_{\min} = \chi_{\text{target}}/\beta_0$, which is the QSL time T_{QSL} for states evolving under an arbitrary time-independent Hamiltonian in the "Heisenberg regime" [43]. We refer to $|\dot\chi| \leqslant |\beta|$ as the QSL constraint. The present work leads to a general definition of T_{QSL}, $\chi(T_{\text{QSL}}) = \chi_{\text{target}} \equiv \int_0^{T_{\text{QSL}}} dt'|\beta(t')|$, for arbitrary time-dependent two-level systems. This definition is consistent with that used in Ref. [44] for a certain class of time-dependent Hamiltonians. Note that the QSL evolution $\chi = \pm\int_0^t dt'\beta(t')$ coincides with $b_z = \dot\varphi/2$, suggesting that the fastest quantum operations are those which tend to minimize $b_z - \dot\varphi/2$, a tendency that is borne out in the examples given below.

The fact that the QSL appears as a simple condition on χ makes the formalism of Eqs. (3) and (4) very effective for designing quantum controls that operate near the QSL. To see how this works for a general $\beta(t)$, note that a simple way to construct a function $\chi(t)$ which obeys the QSL constraint is to first find a function which satisfies the constraint in the case where $\beta(t) = \beta_0$ is a constant. Denoting the latter function $\chi_0(t)$ and defining $B(t) \equiv \int_0^t dt'\beta(t')$, if we choose $\chi(t) = \chi_0(B(t)/\beta_0)$, then $|\dot\chi| = |\beta\chi_0'(B/\beta_0)/\beta_0| \leqslant |\beta|$ automatically follows. Note that all the single-axis driving examples in [35], where the notation there is related to the present by $q = \cos(2\chi)$, can be extended to multiaxis solutions using this trick. Furthermore, if the control field corresponding to χ_0 operates near the QSL, this will also tend to be the case for the one generated by χ. Focusing, then, on the case $\beta(t) = \beta_0$, we can construct controls that operate near the QSL by choosing a $\chi(t)$ which contains parameters that can be tuned to values where $\chi = \pm\beta_0 t$. An important feature of solutions generated from a $\chi(B)$ whose time dependence arises only through B is that the evolution operator is an ordinary function of B and φ, namely,

$$\xi_\pm(B) = \int_0^B dB'\sqrt{1-\chi'^2}\csc(2\chi) \pm \frac{1}{2}\sin^{-1}(\chi') \pm \eta\frac{\pi}{4}, \tag{5}$$

where $\chi'(B) = d\chi/dB$. This fact greatly facilitates the design of a desired evolution since one can directly control the values of u_{11} and u_{21} by adjusting B and φ.

IV. PULSE EXAMPLES

A. Gaussian-like pulses

To illustrate this method of obtaining multiaxis solutions from single-axis ones, consider the example $\chi = -\frac{1}{2}\cos^{-1}(e^{-2\beta_0^2 t^2})$, where $\beta = \beta_0$ and $\eta = 1$, and the QSL constraint is satisfied. Using the method described above, we can extend this to a solution for any $\beta(t)$,

$$\chi = -\tfrac{1}{2}\cos^{-1}\left(e^{-2B(t)^2}\right), \tag{6}$$

which yields the following driving terms:

$$b_x = \dot B\cos\varphi, \quad b_y = \dot B\sin\varphi,$$
$$b_z = \frac{4B^2\dot B}{\sqrt{e^{4B^2} - 4B^2 - 1}} + \dot\varphi/2. \tag{7}$$

The evolution for any B and φ is given by Eqs. (3) and (5). An explicit example is $B = \mu\,\text{erf}(\nu t)/2$ and $\varphi = 0$, yielding a Gaussian and a quasi-Gaussian pulse for b_x and b_z,

$$b_x = \frac{\mu\nu e^{-\nu^2\tau^2}}{\sqrt\pi}, \quad b_z = \frac{\mu^3\nu e^{-\nu^2\tau^2}\text{erf}(\nu\tau)^2/\sqrt\pi}{\sqrt{e^{\mu^2\text{erf}(\nu\tau)^2} - \mu^2\text{erf}(\nu\tau)^2 - 1}}, \tag{8}$$

where $\tau \equiv t - t_0$ and the heights, widths, and centers of these pulses can be controlled by tuning the parameters μ and ν. These pulses and the evolution they produce are shown in Fig. 1, where it is clear that these pulses have a simple, smooth shape.

B. Pulses with arbitrarily many parameters

For a near-QSL pulse example, consider the case

$$\chi = -\beta_0 t[1 + (a_2 t)^2 + (a_4 t)^4 + \cdots + (a_k t)^k]^{-1/k}, \tag{9}$$

where $\beta(t) = \beta_0$ and the a_i are arbitrary constants, k is an even integer, and $\varphi = 0$, $\eta = 1$. The QSL constraint is satisfied regardless of how large k is, so that this χ yields an exact

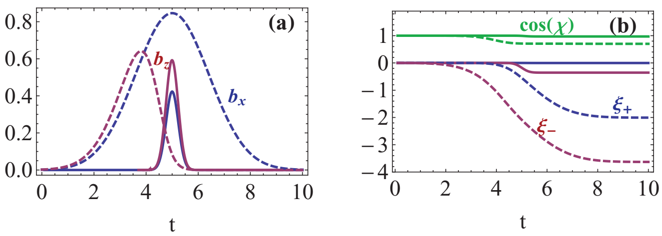

FIG. 1. (Color online) (a) Driving fields from Eq. (8) and (b) corresponding evolution operator parameters for $t_0 = 5$ and $\mu = 1/4, \nu = 3$ (solid lines), $\mu = 3, \nu = 1/2$ (dashed lines).

solution with arbitrarily many parameters a_i. We can make the corresponding control field a pulse by setting $a_k = 4\beta_0/\pi$, so that $\chi \to -\pi/4$ and $b_z \to 0$ as $t \to \infty$. The initial value of the pulse is set by a_2: $b_z(0) = 2a_2\beta_0$. Examples of these pulses are shown in Fig. 2(a). The duration of the pulse approaches $T_{\rm QSL}$ in the limit $a_{i<k} \to 0, k \to \infty$, as can be seen by observing that $\chi \to -\beta_0 t$ in this limit. The substantial amount of tunability in this solution already makes it very attractive for applications in quantum computation such as dynamically corrected gates [32,34,39], where the shape of the pulse is tuned to perform a specific quantum operation while simultaneously suppressing errors.

Using the prescription outlined above, we can extend this solution to the case of nonconstant β:

$$\chi = -B(t)\{1 + [a_2 B(t)]^2 + [a_4 B(t)]^4 + \cdots + [a_k B(t)]^k\}^{-1/k}. \tag{10}$$

This class of pulses can be used to implement quantum operations by tuning $b_z(t)$ for a given choice of $b_x(t)$ and $b_y(t)$. We demonstrate this by designing a fast b_z pulse that, together with b_x, implements a Hadamard gate, a quantum operation that is ubiquitous in the field of quantum information processing and that is equivalent to a π rotation about $\hat{x} + \hat{z}$. First, choose $a_k = 4/\pi$, which ensures that $|u_{11}|,|u_{21}| \to 1/\sqrt{2}$. Supposing that $\varphi = 0$, if we let the system evolve for a time T such that $\int_0^{B(T)} dB' \sqrt{1-\chi'^2}\csc(2\chi) = -5\pi/4$, then the phases of u_{11} and u_{21} will also attain their Hadamard values. Such a b_z pulse is shown in Fig. 2(b) for an oscillatory b_x. From Fig. 2(b), it is evident that b_z quickly sets the magnitudes of u_{11} and u_{21}, while the remainder of the evolution with $b_z \approx 0$ allows their phases to accumulate. As before, the duration of the pulse approaches $T_{\rm QSL}$ as $a_{i<k} \to 0, k \to \infty$. This example illustrates how one can use this formalism to design analytical

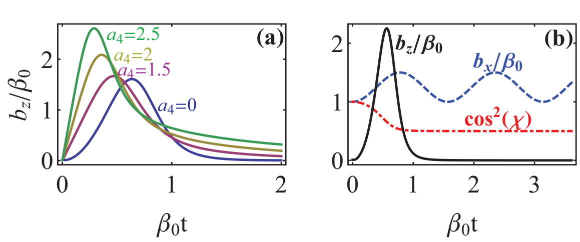

FIG. 2. (Color online) Control field b_z generated by the χ from (a) Eq. (9) with $b_x = \beta_0$, $\varphi = 0$, $k = 6$, $a_2 = 0$, and $a_6 = 4/(\pi\beta_0)$ and (b) Eq. (10) with $b_x = \beta_0(1 + \sin^2(2\beta_0 t)/2)$, $\varphi = 0$, $k = 6$, $a_2 = a_4 = 0$, and $a_6 = 4/\pi$. A Hadamard gate is achieved for a total evolution duration $T = 3.61/\beta_0$.

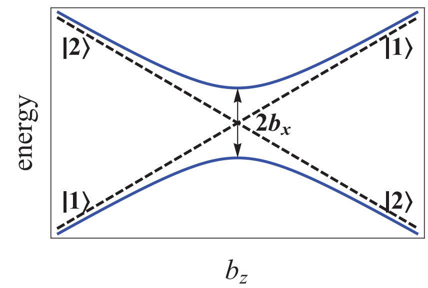

FIG. 3. (Color online) Diabatic and adiabatic energy levels.

controls near the QSL in the presence of additional driving fields.

V. LMSZ INTERFEROMETRY

The present formalism is also natural for designing driving fields that perform controlled LMSZ interferometry and NARP, phenomena which have many applications in quantum control [8–11], state preparation [12,13], and qubit readout [36–38]. (See Refs. [14] and [49–53] and references therein for previous analytical approaches to the LMSZ problem.) The LMSZ problem is generally set up as follows. Define the eigenstates of σ_z to be $|1\rangle$ and $|2\rangle$ and set $\varphi = 0$ so that $\beta = b_x$; when $|b_z| \gg |b_x|$, these states are approximate energy eigenstates. A nonzero b_x produces an anticrossing with an energy gap of $2b_x$ (see Fig. 3) which may be time dependent. Now suppose that we drive b_z through the anticrossing, starting from some large negative value at $t = 0$ up to a large positive value at $t = T$. Assuming that the system is initially prepared in state $|1\rangle$ at time $t = 0$, the probability $P_2(T)$ for the system to be in state $|2\rangle$ at time $t = T$ is

$$P_2(T) = |u_{21}(T)|^2 = \sin^2[\chi(T)]. \tag{11}$$

The fact that this depends only on $\chi(T)$ demonstrates the suitability of the present formalism for the LMSZ problem. If we choose χ such that $\chi(0) = 0$ and $\chi(T) = 0$, then we achieve a perfect LMSZ transition: the system is driven through the anticrossing and returns to state $|1\rangle$ with probability 1. On the other hand, we may choose $\chi(T) = \pi/2$, in which case the system undergoes NARP and ends up in state $|2\rangle$ after being driven through the anticrossing. Other values of $\chi(T)$ lead to superpositions of $|1\rangle$ and $|2\rangle$. We may also consider LMSZ interferometry, where the system is driven through the anticrossing periodically, and the resulting time-averaged probabilities of being in state $|1\rangle$ or $|2\rangle$ after many periods is again largely determined by $\chi(T)$, as we will see. In choosing a $\chi(t)$ for the LMSZ problem, we must impose appropriate initial conditions. For simplicity, we focus on the case $b_z(0) = -\infty$, $b_z(T) = \infty$, for which we need $\ddot{\chi}(0) < 0$, $\ddot{\chi}(T) > 0$; the analysis can be extended straightforwardly to the case where b_z is finite at $t = 0, T$.

For constant b_x, a simple example which satisfies these boundary conditions and the QSL constraint is

$$\chi = b_x t - \frac{ab_x T}{2}t^2 + \frac{ab_x}{3}t^3, \tag{12}$$

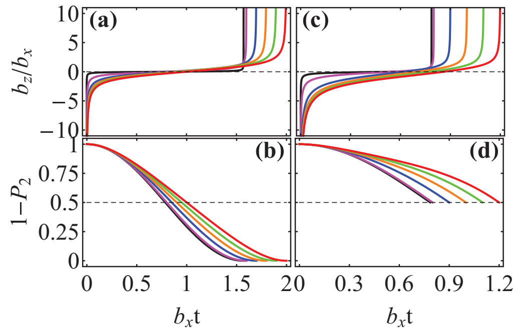

FIG. 4. (Color online) (a) Control field and (b) NARP probability from Eqs. (12), (11), and (4) with $\chi(T)=\pi/2$ and $b_xT=\pi/2$, 1.6, 1.7, 1.8, 1.9, and 2 and (c, d) $\chi(T)=\pi/4$ and $b_xT=\pi/4$, 0.8, 0.9, 1, 1.1, and 1.2.

where choosing $0\leqslant a\leqslant 16/(3T^2)$ ensures that the b_z from Eq. (3) is finite in the interval $t\in(0,T)$, and $\eta=-1$. This χ saturates the QSL constraint when $a=0$, implying that b_z will implement near-QSL evolution for small a. To achieve a target $\chi(T)$, set $t=T$ in Eq. (12) and solve for a: $a(T)=6[b_xT-\chi(T)]/(b_xT^3)$. Plugging this into Eqs. (12) and (4) yields a family of driving fields b_z parametrized by T that achieve the desired evolution for any $\chi(T)\in(0,\pi/2]$; some of these are shown in Fig. 4 along with the corresponding NARP probabilities. The restrictions on $a(T)$ impose bounds on T: $\chi(T)\leqslant b_xT\leqslant 9\chi(T)$. The upper bound is particular to Eq. (12), while the lower bound is the familiar, universal QSL and gives rise to the step-like curves in Figs. 4(a) and 4(c). These curves reveal that the desired LMSZ transition is achieved as quickly as possible by first driving b_z to 0 very rapidly, allowing the system to evolve for a time $T\lesssim T_{\rm QSL}$ and then driving b_z quickly up to its final value (see also Ref. [46]). In addition to NARP, these near-QSL driving fields could be important for LMSZ-based generation of entanglement in superconducting qubits [10], where fidelities are often limited by short relaxation times.

In the context of LMSZ interferometry, the formalism of Eqs. (3) and (4) yields an exact formula for LMSZ interference patterns. To show this, we begin by constructing a periodic driving field b_z of period $2T$, where $\chi(t)$ determines the first half of one period and $\chi_2(t)=\chi(2T-t)$ the second half, corresponding to b_z retracing its path. Using Eq. (3), we find the evolution after one full period:

$$
\begin{aligned}
u_{11}(2T)&=e^{2i\xi_0(T)}\cos\left(2\chi(T)\right),\\
u_{21}(2T)&=-i\sin\left(2\chi(T)\right),
\end{aligned}
\tag{13}
$$

where $\xi_0\equiv(\xi_++\xi_-)/2$ and we have assumed that $\dot\chi(T)=-\eta\beta(T)$ for simplicity. From this expression, it is straightforward to compute the time-averaged probability of being in the excited state $|2\rangle$ after many periods:

$$
\bar{\mathcal{P}}_2=[2+2\cot^2\left(2\chi(T)\right)\sin^2\left(2\xi_0(T)\right)]^{-1}. \tag{14}
$$

Thus, we see that the present formalism readily produces a general, exact, analytic formula for $\bar{\mathcal{P}}_2$, whereas analytic expressions for this important quantity typically require several approximations [5]. This function takes values in the range $[0,1/2]$, where $\bar{\mathcal{P}}_2=1/2$ for $\chi(T)=\pi/4$, while $\bar{\mathcal{P}}_2=0$ for $\chi(T)=\pi/2$. This is to be expected since $\chi(T)=\pi/4$ corresponds to a 50:50 "beam splitter," while $\chi(T)=\pi/2$ ensures that the system remains in the ground state after every sweep through the anticrossing. In the context of charge qubits where states $|1\rangle$ and $|2\rangle$ correspond to an electron being in either the left or the right dot of a tunnel-coupled double quantum dot, the case $\bar{\mathcal{P}}_2=0$ can be interpreted as coherent destruction of tunneling [47,48] since the electron becomes localized in one dot. For more generic values of $\chi(T)$, $\bar{\mathcal{P}}_2$ is modulated by the phase $\xi_0(T)$, which can produce interference fringes as control parameters are adjusted, as shown in Fig. 5 for the example from Eq. (12) with $\chi(T)=\pi/2.1$. As T is varied, an interference pattern emerges in which the peaks of the pattern sharpen and eventually disappear as $\chi(T)$ approaches $\pi/2$. Interestingly, Fig. 5 reveals a peak at the QSL time $T=T_{\rm QSL}=\pi/(2.1b_x)$; this is generally the case since at the QSL, $|\dot\chi|=|\beta|$, so that $\xi_0(T_{\rm QSL})=0$. This leads to the surprising conclusion that if we choose $\chi(T)=\pi/2$ in order to trap the system in state $|2\rangle$, then driving very close to the QSL may not be ideal since small deviations away from $\chi(T)=\pi/2$ will produce the peak at $T=T_{\rm QSL}$ and, hence, large uncertainty in the state of the system.

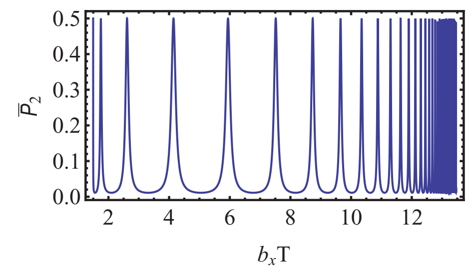

FIG. 5. (Color online) Time-averaged excited-state probability $\bar{\mathcal{P}}_2$ from Eq. (14) with a periodic driving field generated by Eq. (12) with $\chi(T)=\pi/2.1$ and half-period T. The nonmonotonicity in the fringe spacing reflects the nonmonotonicity of Eq. (12) at larger values of T.

VI. CONCLUSIONS

In conclusion, a general formalism for deriving exactly solvable time-dependent two-level quantum systems has been presented. This formalism can vastly increase the number of known exact solutions for physical Hamiltonians, as has been demonstrated with explicit examples. These examples show that this theory can be a powerful tool in the design of control pulses both for quantum computation and for precise LMSZ interferometry near the QSL.

ACKNOWLEDGMENTS

I thank Michael Berry, Lev Bishop, Łukasz Cywiński, and Sophia Economou for helpful discussions. I also thank Gerhard Hegerfeldt for useful comments. This work was supported by LPS-NSA and IARPA.

APPENDIX

In this Appendix, we derive Eqs. (3) and (4) in the text. The general form of the Hamiltonian and its corresponding evolution operator are given in Eqs. (1) and (2). The evolution operator obeys a Schrödinger equation whose form can be made compact by transforming to a rotating frame: $v_{11} = e^{i\int_0^t dt' b_z(t')} u_{11}$, $v_{21} = e^{-i\int_0^t dt' b_z(t')} u_{21}$. Defining $\beta e^{i\varphi} \equiv b_x + i b_y$ and $\alpha(t) \equiv 2\int_0^t dt' b_z(t') - \varphi(t)$, we have

$$\dot{v}_{11} = -i\beta e^{i\alpha} v_{21}, \quad \dot{v}_{21} = -i\beta e^{-i\alpha} v_{11}. \tag{A1}$$

Here, it is manifest that the evolution operator in the rotating frame depends on only two real functions, α and β. We must further specify b_z to return to the laboratory frame, but this choice can be made after the evolution operator is computed in the rotating frame. In what follows, I show that one can systematically find analytical solutions with either α or β chosen as desired; although one cannot choose both α and β at will (if this were the case, all two-state problems would be analytically solvable), we will see that one still has a large amount of control over the features of the second, unspecified function.

For concreteness, we suppose that $\beta(t)$ is chosen at the outset [the formalism can easily be modified to fix $\alpha(t)$ instead]. While we cannot then find analytical solutions for arbitrary α, there exists a different parametrization of the Hamiltonian in which α is replaced with a new function, $\kappa_I(t)$, such that one can systematically generate an analytical expression for the evolution operator for arbitrary choices of β and κ_I. To see this, first express the rotating-frame evolution operator in terms of some complex $\kappa(t)$:

$$v_{11} = e^{-i\int_0^t dt'\beta(t')e^{\kappa(t')}}, \quad v_{21} = -i\eta e^{-i\int_0^t dt'\beta(t')e^{-\kappa(t')}}, \tag{A2}$$

with $\eta = \pm 1$. This choice of parametrization is motivated by observing that we can combine the two equations in (A1) to obtain $\beta^2 = -(\dot{v}_{11}/v_{11})(\dot{v}_{21}/v_{21})$, which generally implies $\dot{v}_{11}/v_{11} = -i\beta e^{\kappa}, \dot{v}_{21}/v_{21} = -i\beta e^{-\kappa}$ for some complex κ. The fact that this is true in general can be seen by noting that for $\beta \neq 0$, any complex function can be expressed as $-i\beta e^{\kappa}$ for some complex function κ, so that we may therefore express $\dot{v}_{11}/v_{11}$ in this way. $\beta^2 = -(\dot{v}_{11}/v_{11})(\dot{v}_{21}/v_{21})$ then implies $\dot{v}_{21}/v_{21} = -i\beta e^{-\kappa}$. This argument does not hold when $\beta = 0$, however, in this case we find $\dot{v}_{11} = 0 = \dot{v}_{21}$, which is consistent with Eq. (A1). This analysis is thus completely general and applies to any solution of the Schrödinger equation. Consistency between Eq. (A2) and Eq. (A1) requires

$$\alpha(t) = -i\kappa(t) + \eta\frac{\pi}{2} - 2\int_0^t dt'\beta(t')\sinh\kappa(t'), \tag{A3}$$

which should be interpreted as follows. For any choice of a complex $\kappa(t)$ and real $\beta(t)$ such that the $\alpha(t)$ computed from Eq. (A3) is real, the evolution operator obtained from Eq. (A2) is the exact solution for this α and β. Writing $\kappa = \kappa_R + i\kappa_I$ and imposing $\mathrm{Im}(\alpha) = 0$ determines κ_R in terms of κ_I: $\kappa_R = -2\tanh^{-1}\tan(\chi + \pi/4)$, with

$$\chi(t) \equiv \int_0^t dt'\beta(t')\sin(\kappa_I(t')). \tag{A4}$$

This leads to an expression for α that is real for any κ_I:

$$\alpha = \kappa_I + \eta\frac{\pi}{2} - 2\int_0^t dt'\beta(t')\cos\kappa_I(t')\cot[2\chi(t')]. \tag{A5}$$

While this parametrization has the nice feature that κ_I can be chosen freely, one drawback is that one must then perform the integration in Eq. (A4), making it harder to relate the features of κ_I to the driving field $\dot{\alpha}$. We can avoid this by specifying χ directly, but at the expense of now having to choose functions $\chi(t)$ that obey the QSL constraint, $|\dot{\chi}| \leqslant |\beta|$, which arises directly from Eq. (A4). Solving Eq. (A4) for κ_I in terms of χ, it is straightforward to turn the above expressions for the evolution operator into expressions which depend on χ rather than κ_I. The resulting laboratory-frame evolution operator and driving fields are given in Eqs. (3) and (4).

[1] L. Landau, Phys. Z. Sowjetunion **2**, 46 (1932).
[2] C. Zener, Proc. R. Soc. Lond. A **137**, 696 (1932).
[3] E. C. G. Stückelberg, Helv. Phys. Acta **5**, 369 (1932).
[4] E. Majorana, Nuovo Cimento **9**, 43 (1932).
[5] S. Shevchenko, S. Ashhab, and F. Nori, Phys. Rep. **492**, 1 (2010).
[6] W. H. Zurek, U. Dorner, and P. Zoller, Phys. Rev. Lett. **95**, 105701 (2005).
[7] M. S. Rudner, A. V. Shytov, L. S. Levitov, D. M. Berns, W. D. Oliver, S. O. Valenzuela, and T. P. Orlando, Phys. Rev. Lett. **101**, 190502 (2008).
[8] J. R. Petta, H. Lu, and A. C. Gossard, Science **327**, 669 (2010).
[9] H. Ribeiro, J. R. Petta, and G. Burkard, arXiv:1210.1957.
[10] C. M. Quintana, K. D. Petersson, L. W. McFaul, S. J. Srinivasan, A. A. Houck, and J. R. Petta, Phys. Rev. Lett. **110**, 173603 (2013).
[11] J. Zhang, J. H. Shim, I. Niemeyer, T. Taniguchi, T. Teraji, H. Abe, S. Onoda, T. Yamamoto, T. Ohshima, J. Isoya *et al.*, Phys. Rev. Lett. **110**, 240501 (2013).
[12] Y. Wu, I. M. Piper, M. Ediger, P. Brereton, E. R. Schmidgall, P. R. Eastham, M. Hugues, M. Hopkinson, and R. T. Phillips, Phys. Rev. Lett. **106**, 067401 (2011).
[13] R. T. Brierley, C. Creatore, P. B. Littlewood, and P. R. Eastham, Phys. Rev. Lett. **109**, 043002 (2012).
[14] N. Malossi, M. G. Bason, M. Viteau, E. Arimondo, R. Mannella, O. Morsch, and D. Ciampini, Phys. Rev. A **87**, 012116 (2013).
[15] N. Rosen and C. Zener, Phys. Rev. **40**, 502 (1932).
[16] S. L. McCall and E. L. Hahn, Phys. Rev. **183**, 457 (1969).
[17] S. E. Economou, L. J. Sham, Y. Wu, and D. G. Steel, Phys. Rev. B **74**, 205415 (2006).
[18] A. Greilich, S. E. Economou, S. Spatzek, D. R. Yakovlev, D. Reuter, A. D. Wieck, T. L. Reinecke, and M. Bayer, Nat. Phys. **5**, 262 (2009).
[19] E. Poem, O. Kenneth, Y. Kodriano, Y. Benny, S. Khatsevich, J. E. Avron, and D. Gershoni, Phys. Rev. Lett. **107**, 087401 (2011).
[20] A. Bambini and P. R. Berman, Phys. Rev. A **23**, 2496 (1981).
[21] A. Bambini and M. Lindberg, Phys. Rev. A **30**, 794 (1984).
[22] F. T. Hioe, Phys. Rev. A **30**, 2100 (1984).
[23] J. Zakrzewski, Phys. Rev. A **32**, 3748 (1985).
[24] M. S. Silver, R. I. Joseph, and D. I. Hoult, Phys. Rev. A **31**, 2753(R) (1985).
[25] E. J. Robinson, Phys. Rev. A **31**, 3986 (1985).
[26] A. M. Ishkhanyan, J. Phys. A **33**, 5539 (2000).

[27] L. Carmel and A. Mann, Phys. Rev. A **61**, 052113 (2000).
[28] E. S. Kyoseva and N. V. Vitanov, Phys. Rev. A **71**, 054102 (2005).
[29] N. V. Vitanov, New J. Phys. **9**, 58 (2007).
[30] F. T. Hioe, in *Advances in Chemical Physics: Lasers, Molecules, and Methods* (Wiley, New York, 2007), p. 73.
[31] S. E. Economou, Phys. Rev. B **85**, 241401(R) (2012).
[32] F. Motzoi, J. M. Gambetta, P. Rebentrost, and F. K. Wilhelm, Phys. Rev. Lett. **103**, 110501 (2009).
[33] J. M. Chow, L. DiCarlo, J. M. Gambetta, F. Motzoi, L. Frunzio, S. M. Girvin, and R. J. Schoelkopf, Phys. Rev. A **82**, 040305(R) (2010).
[34] J. M. Gambetta, F. Motzoi, S. T. Merkel, and F. K. Wilhelm, Phys. Rev. A **83**, 012308 (2011).
[35] E. Barnes and S. Das Sarma, Phys. Rev. Lett. **109**, 060401 (2012).
[36] J. R. Petta, A. C. Johnson, J. M. Taylor, E. A. Laird, A. Yacoby, M. D. Lukin, C. M. Marcus, M. P. Hanson, and A. C. Gossard, Science **309**, 2180 (2005).
[37] S. Foletti, H. Bluhm, D. Mahalu, V. Umansky, and A. Yacoby, Nat. Phys. **5**, 903 (2009).
[38] B. M. Maune, M. G. Borselli, B. Huang, T. D. Ladd, P. W. Deelman, K. S. Holabird, A. A. Kiselev, I. Alvarado-Rodriguez, R. S. Ross, A. E. Schmitz *et al.*, Nature **481**, 7381 (2012).
[39] X. Wang, L. S. Bishop, J. P. Kestner, E. Barnes, K. Sun, and S. Das Sarma, Nat. Commun. **3**, 997 (2012).
[40] L. Mandelstam and I. Tamm, J. Phys. (USSR) **9**, 249 (1945).
[41] K. Bhattacharyya, J. Phys. A: Math. Gen. **16**, 2993 (1983).
[42] N. Margolus and L. B. Levitin, Physica D **120**, 188 (1998).
[43] V. Giovannetti, S. Lloyd, and L. Maccone, Phys. Rev. A **67**, 052109 (2003).
[44] T. Caneva, M. Murphy, T. Calarco, R. Fazio, S. Montangero, V. Giovannetti, and G. E. Santoro, Phys. Rev. Lett. **103**, 240501 (2009).
[45] M. G. Bason, M. Viteau, N. Malossi, P. Huillery, E. Arimondo, D. Ciampini, R. Fazio, V. Giovannetti, R. Mannella, and O. Morsch, Nat. Phys. **8**, 147 (2012).
[46] G. C. Hegerfeldt, arXiv:1305.6403.
[47] F. Grossmann, T. Dittrich, P. Jung, and P. Hänggi, Phys. Rev. Lett. **67**, 516 (1991).
[48] J. Stehlik, Y. Dovzhenko, J. R. Petta, J. R. Johansson, F. Nori, H. Lu, and A. C. Gossard, Phys. Rev. B **86**, 121303(R) (2012).
[49] M. V. Berry, Proc. R. Soc. Lond. A **429**, 61 (1990).
[50] R. Lim and M. Berry, J. Phys. A: Math. Gen. **24**, 3255 (1991).
[51] N. V. Vitanov and K.-A. Suominen, Phys. Rev. A **59**, 4580 (1999).
[52] M. V. Berry, J. Phys. A **42**, 365303 (2009).
[53] A. Ruschhaupt, X. Chen, D. Alonso, and J. G. Muga, arXiv:1206.1691.